# Multiway Uniform Combline Directional Couplers for Microwave Frequencies

SAIFUL ISLAM

*Abstract* —An improved optimization technique for multiway uniform forward directional couplers is presented using a previously published matrix theory of coupled transmission lines. With the help of this computer optimization method, microwave mode-interference combline directional couplers having an arbitrary number of lines can be designed for arbitrary power distribution. Theoretical designs ranging from two-way to nine-way couplers have been tested with success. The observed behavior of some of these couplers is briefly discussed. Typically these couplers exhibited octave bandwidth. A five-way design example of an equal power splitting combline coupler has been fabricated using an open microstripline configuration for operation within 1.6–3.2 GHz. The measured characteristics show good agreement with the computed values.

## I. Introduction

In a MICROWAVE forward directional coupler power in both the coupled and the excited line flow in the same direction, in contrast to the well-known backward or reverse couplers [1]–[6], where power in the coupled line flows in opposite direction. It is known that coupled planar microstrip comblines [7], [8], [10] produce forward coupling [7], [8]. This fact has been supported by the results of the experimental combline directional couplers shown in [7], [8], and [10]–[12]. A directional coupler using comblines having unaltered line parameters and interline coupling along the coupled length is referred to here as a uniform combline directional coupler, or UCDC.

This paper is concerned with the design and fabrication of multiway UCDC's (having $N$ coupled lines) rather than two-way UCDC's only. Fig. 1 shows a fabricated five-way UCDC. From [10] and [11] it may be observed that the individual lines of a UCDC have different phase velocities and uncoupled impedances. Coupling between any two adjacent lines in such a coupler depends on (i) the difference in phase velocities and (ii) the interline coupling capacitance. The interpretation in terms of normal modes [12] is that coupling occurs due to interference of the normal modes. As a result these couplers may be termed mode-interference couplers. This paper deals with the design of this type of coupler by computer optimization.

In a previous work [11] computer optimization of $2N$ variables with a steepest descent algorithm was used for designing $N$-way UCDC's. This work [11] presented a successful design of a five-way UCDC along with good experimental results. While following this method for a five-way UCDC, a number of difficulties were encountered by the author. These are: (i) the different values of optimized error function for different starting sets of variables; (ii) the time-consuming task of the random search technique [11] for obtaining a starting set of variables; and (iii) the requirement of several inspection and manual interruptions for changing a parameter $p$ [11] at different stages of the optimization. The main cause of the observed uncertainty seemed to be the fact that out of $2N$ variables the upper and lower bounds could not be fixed for the first $N$ variables. Also, for the remaining $N$ variables, the limits could not be narrowed properly in order to direct the optimization towards the desired direction. As a result sometimes it was difficult to avoid or get out of a local minimum.

From this observation it was understood that an improved optimization method is necessary in order to reduce and, if possible, eliminate the uncertainty. It was thought to be worthwhile to look for (i) a different set of variables which do not require random search and (ii) a different optimization algorithm having better search techniques in order to achieve the desired improvements.

A search was therefore made for that approach to the design. In this paper, an improved optimization method is presented using a different set of variables which always ensures practical realizability. This new set of variables has one element less than the set used in the previous work [11] and does not require any normalization of the variables.

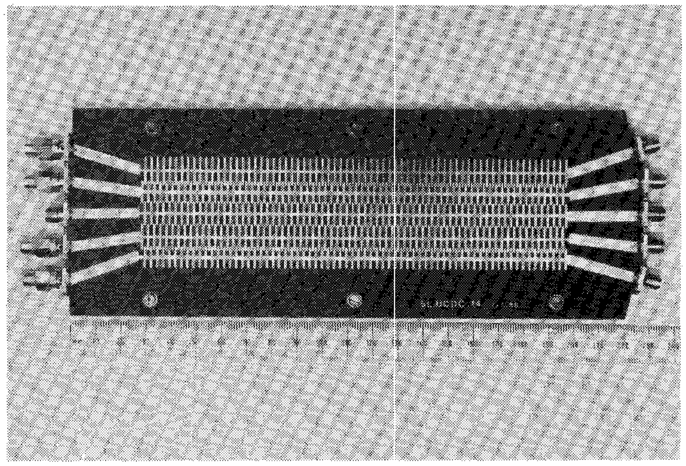

Fig. 1. Photograph of an equal power splitting five-way UCDC.

Manuscript received July 29, 1987; revised December 16, 1987.
The author was with the Cambridge University Engineering Department, Cambridge, U.K. He is now with the Electrical and Electronic Engineering Department, Bangladesh University of Engineering and Technology, Dhaka 1000, Bangladesh.
IEEE Log Number 8820437.

The optimization with the new set of variables has been found to be not critically dependent on the starting values. By using the available library optimization subroutines of a mainframe computer, the overall design work has been made efficient and easy to use. The method has been found to work without failure for two-line up to nine-line couplers.

## II. Power and Phase Characteristics of an $N$-Line UCDC

Consider the transmission line model for the $N$ coupled lines of an $N$-way UCDC. Assuming that only forward waves are propagating and scattering in the $z$ direction, it is possible to write [12]

$$\frac{d}{dz}\boldsymbol{a}(z) = -jJ\boldsymbol{a}(z). \tag{1}$$

In this equation, the $N$-row forward wave amplitude vector $\boldsymbol{a}(z)$ is

$$\boldsymbol{a}(z) = (1/2)\left(\boldsymbol{R}_t^{-1/2}\boldsymbol{v} + \boldsymbol{R}_t^{1/2}\boldsymbol{i}\right). \tag{2}$$

The vectors $\boldsymbol{v}$ and $\boldsymbol{i}$ are formed with the voltages and currents, respectively, on the lines, and $\boldsymbol{R}_t$ is the diagonal termination impedance matrix [11], with $R_{ti}$ as the diagonal elements. The $\boldsymbol{J}$ matrix in (1) is the wave propagation matrix [12] of the coupler and is related to the inductance and capacitance matrices [11] of the coupler as shown in Appendix I. For lossless lines the $\boldsymbol{J}$ matrix is real and symmetric and for planar structure (with nearest neighbor interaction) this is a tridiagonal matrix.

The eigenvalues of the wave propagation matrix $\boldsymbol{J}$ are the mode propagation constants $\beta_i$ $(i = 1,2,\cdots,N)$ on the lines so that

$$\boldsymbol{QJQ}^t = \boldsymbol{\beta}. \tag{3}$$

The matrix $\boldsymbol{\beta}$ [11], [12] is the diagonal matrix containing the mode propagation constants $\beta_i$'s as the diagonal elements, and the $\boldsymbol{Q}$ matrix [10]–[12] is the orthogonal modal matrix containing the eigenvectors of the symmetric matrix $\boldsymbol{J}$. For lossless lines, the elements of the orthogonal modal matrix $\boldsymbol{Q}$ are real. We denote the orthonormal row vectors of $\boldsymbol{Q}$ as $\boldsymbol{q}_i$ $(i = 1,2,\cdots,N)$ and the orthonormal column vectors of the same matrix as $\boldsymbol{p}_j$ $(j = 1,2,\cdots,N)$. Here, the vectors $\boldsymbol{q}_i$ are the eigenvectors of the $\boldsymbol{J}$ matrix.

The input output relationship of a UCDC may be written [9], [10] as

$$\boldsymbol{b}_o = \boldsymbol{S}_{oi}\boldsymbol{a}_i \tag{4}$$

where $\boldsymbol{b}_o = (b_{o1}, b_{o2}, \cdots, b_{oN})^t$ is the vector containing the complex wave amplitudes at the output ports, $\boldsymbol{a}_i = (a_{i1}, a_{i2}, \cdots, a_{iN})^t$ is the vector containing the input wave amplitudes, and $\boldsymbol{S}_{oi}$ is the forward scattering matrix of the coupler.

The equation for the forward scattering matrix of a single-section UCDC was shown in [9]–[12]. A convenient form of this equation is

$$\boldsymbol{S}_{oi} = \boldsymbol{Q}^t\boldsymbol{E}^{-1}\boldsymbol{Q} = \boldsymbol{Q}^t\{\exp(j(f/f_o)L_o\boldsymbol{\beta})\}^{-1}\boldsymbol{Q} \tag{5}$$

where $L_o$ is the coupled length of the coupler and $f_o$ is the normalizing frequency. This equation enables one to obtain the forward scattering matrix of a UCDC at any frequency $f$.

Taking unit excitation at the input port of the $k$th line and using (4) and (5), we can write the output wave amplitude of the $i$th line as

$$b_{oi} = \boldsymbol{p}_k^t\boldsymbol{E}^{-1}\boldsymbol{p}_i = \boldsymbol{b}_{oi\mathrm{R}} + j\boldsymbol{b}_{oi\mathrm{I}}. \tag{6}$$

Here the subscript R is used for the real part and I for the imaginary part.

The power at the output of the $i$th line is then

$$P_{oi} = b_{oi}b_{oi}^* = \boldsymbol{p}_k^t\boldsymbol{E}^{-1}\boldsymbol{p}_i\boldsymbol{p}_k^t\boldsymbol{E}\boldsymbol{p}_i \tag{7}$$

since $(\boldsymbol{E}^{-1})^* = \boldsymbol{E}$. Here due to conservation of power,

$$\sum_{i=1}^{N} P_{oi} = P_{in} = 1. \tag{8}$$

The amplitude $b_{oi}$ at the output port of the $i$th line may now be obtained at any frequency $f$ by using (6). The power in dB $\{10\log(P_{oi}/P_{in})\}$ against frequency characteristics may then be obtained using (7).

The absolute phase of the $i$th line is

$$\Phi_{oi} = \tan^{-1}\{b_{oi\mathrm{I}}/b_{oi\mathrm{R}}\}. \tag{9}$$

The relative phase of the $i$th line with respect to the $k$th line is

$$\Phi_{ri} = \Phi_{oi} - \Phi_{ok} = \tan^{-1}\frac{(b_{oi\mathrm{I}}b_{ok\mathrm{R}} - b_{oi\mathrm{R}}b_{ok\mathrm{I}})}{(b_{oi\mathrm{R}}b_{ok\mathrm{R}} + b_{oi\mathrm{I}}b_{ok\mathrm{I}})}. \tag{10}$$

It may be mentioned here that increasing the coupled length brings down the frequency at which coupling reaches the required value (i.e., the characteristics are shifted towards left) and conversely when the length is decreased. The same result (i.e., the characteristics) can be obtained by scalar multiplication of the matrix $\boldsymbol{J}$ by a factor instead of changing the length.

## III. The Technique of Designing a "Single-Section" UCDC

It may be observed from the last section that by knowing the elements of the tridiagonal (for nearest neighbor interaction) wave propagation matrix $\boldsymbol{J}$ and the coupled length of a coupler, one can obtain the scattering matrix (which means the characteristics) of a UCDC. Besides this, one can obtain the line parameters of a UCDC from the $\boldsymbol{J}$ matrix, as shown in Appendix I. The wave propagation matrix is thus the key to the analysis and realization of the couplers using this technique. For convenience, a $2N$-dimensional vector $\boldsymbol{e}$ is now formed with the diagonal elements of the $\boldsymbol{J}$ matrix as the first $N$ elements, with the off-diagonal elements of the same matrix as the next $N-1$ elements and the coupled length as the last element. The above discussion makes it clear that a coupler with nearest neighbor interaction is uniquely specified by specifying this $\boldsymbol{e}$ vector.

Usually the design specifications of a coupler are the wave amplitudes (or the power levels) and the relative phase (sometimes phase may not be important) of the output ports, for unit excitation. Unfortunately no success has yet been achieved in establishing an analytical method to determine the wave propagation matrix from this information only. The forward scattering matrix relation of (5) indicates that without knowing the total scattering matrix, the task of obtaining the wave propagation matrix is not easy. As a result the required wave propagation matrix is obtained through the process of numerical optimization of a set of variables by a computer.

In this optimization process, using a suitable set of variables, an error function is formed by comparing the computed characteristics with the required references within the operating band of frequencies. The error function is then minimized using computer methods by varying the set of variables.

### *A. Set of Variables for Optimization*

For an optimization-based design, the choice of the set of variables may influence the optimization significantly. It is preferable that the set of variables uniquely specify a coupler. Here, the $\boldsymbol{e}$ vector is chosen as the set of variables since this uniquely specifies a coupler. For an $N$-line coupler the $\boldsymbol{e}$ vector is $\boldsymbol{e}^t = (c_1, c_2, \cdots, c_N, d_1, d_2, \cdots, d_{N-1}, L_o)$; where $c_i$ are the diagonal elements and $d_i$ are the off-diagonal terms of the tridiagonal matrix $\boldsymbol{J}$.

In this set of variables the coupled length $L_o$ is not an essential element but it helps to expedite the optimization process. It may be observed that the $\boldsymbol{e}$ vector has $2N$ variables compared to the $2N+1$ variables of the previous work [11].

It is necessary to specify the upper and lower limits for each of the elements of the set of variables in order to (i) save computation time, (ii) avoid undesirable local minima, and (iii) avoid unrealizable parameters. The limits are set such that the first $N$ elements of $\boldsymbol{e}$ are always $+ve$, the next $N-1$ elements are always $-ve$, and the last element is always $+ve$.

### *B. Reference Power Level*

Consider the example of an $N$-line equal power splitting coupler with unit excitation at the input port (other distributions may be chosen). Assuming no loss within the coupler, the power at each of its output ports is $1/N$ within the frequency band of operation. The assumed ideal characteristics for reference purposes is then a straight line at $1/N$ within the operating frequency range $f_1$ to $f_2$. We denote this as the reference power characteristics for the individual lines ($P_{ri}$).

### *C. Error Function for Optimization*

At first the area between the reference level ($P_{ri}$) and the computed characteristics ($P_i(f)$) within the specified band of frequencies is computed for each line. The area for all the lines in a coupler is then summed up to form the error function $E$, which is a function of $\boldsymbol{e}$. This means

$$E(\boldsymbol{e}) = \sum_{i=1}^{N} u_i E_i \tag{11}$$

where $u_i$ is the $+ve$ weighting factor and $E_i$ is the error area of the power characteristics for the $i$th line within the frequency range $f_1$ to $f_2$. Thus $E_i$ is

$$E_i(\boldsymbol{e}) = \int_{f_1}^{f_2} |P_i(f) - P_{ri}|\, df \tag{12}$$

Here, the error function has been shown for power optimization only. However, if the phase optimization is simultaneously required, then the phase error function is to be added with the power error function in order to obtain the total error function. An appropriate positive weight factor multiplier with each quantity is then required before addition.

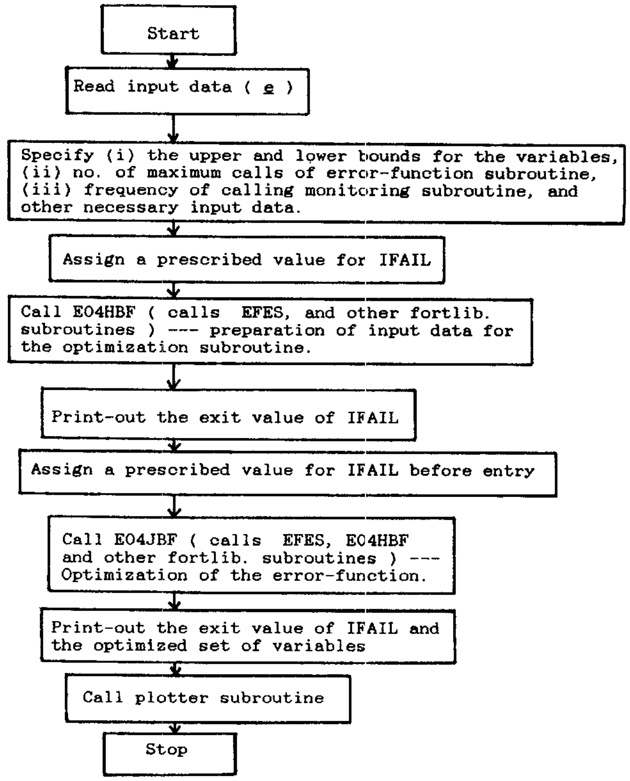


Fig. 2. Flowchart showing the sequences of the main program for the optimization work with the mainframe computer using NAG Fortran library subroutines. Here, EFES is the error function evaluating subroutine as indicated in Fig. 3 and IFAIL is the error indicator [13]

## IV. The Optimization Technique

The computation work has been divided into two parts, i.e., (i) optimization of the error function and (ii) evaluation of the error function. For the computer a subroutine program was prepared for the second part and a main program was prepared for the first part. Programs were prepared in Fortran 77 for running in the mainframe computer (IBM 3081) at Cambridge. The NAG (Numerical Algorithms Group, Oxford, U.K.) library subroutines available in this computer were of great help in performing this complicated and large-dimensional computation.

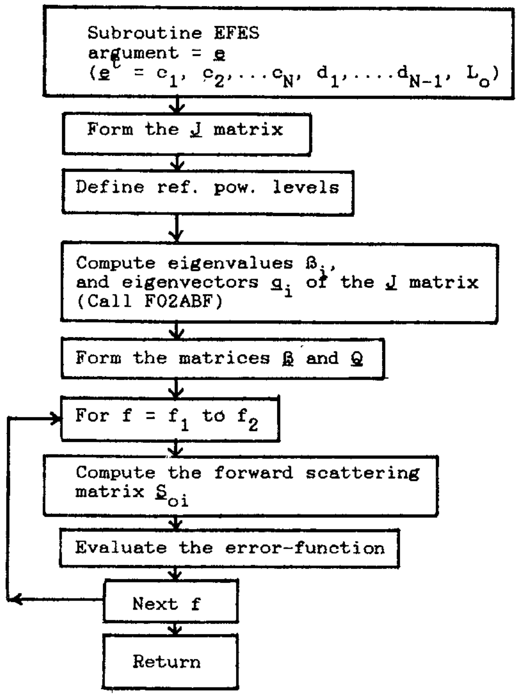


Fig. 3. Flowchart showing the various stages of computations in the error function evaluating subroutine program (EFES) using the $e$ vector as the set of variables. $f$ is frequency, $f_1$ is the lower band-edge frequency, and $f_2$ is the upper band-edge frequency.

### *A. Optimization of the Error Function Using Quasi-Newton-Algorithm-Based NAG Subroutines*

For the optimization of the error function, the programming sequences are presented in Fig. 2. The actual optimization work is done by the NAG subroutine E04JBF [13], which is based on quasi-Newton algorithm [15]. This subroutine is generally used for finding an unconstrained minimum of a function of several variables subject to the fixed upper and lower boundaries on the variables [13].

The error function evaluating subroutine (EFES) may be called several thousand times by the subroutine E04JBF. The number of calls depends on the number of variables $K$ and on the starting point. The maximum number of calls is limited by the program up to $40K(K+5)$ times [13]. Clearly a considerable amount of the computation time is spent in evaluating the error function. It is therefore necessary to prepare the subroutine EFES efficiently so that it takes minimum possible computation time.

At the beginning of the optimization work the program is run for a short time (say 50 sec for a five-way UCDC) and the power plots of the output ports of the coupler are obtained using the new $\boldsymbol{e}$. This enables one to understand whether the optimization program is functioning properly or not.

### *B. Evaluation of the Error Function*

The different steps of computations for evaluating the error function are shown in the flowchart of Fig. 3. For computing the eigenvalues and eigenvectors of the $\boldsymbol{J}$ matrix, the available NAG subrouting F02ABF [14] was used. The error function evaluating subroutine EFES calls the NAG subroutine F02ABF (for obtaining the eigenvalues and the eigenvectors of $\boldsymbol{J}$) once every time the subroutine EFES itself is called by the "optimization subroutine program" or the main program.

## V. Obtaining a Starting Set of Variables for Optimization

At first an $\boldsymbol{e}$ is formed by (a) assuming equal values of $c_i$ (the diagonal elements of $\boldsymbol{J}$), (b) assuming the negative off-diagonal elements $d_i$ in the ratio of desired powers at the output ports, and (c) assuming a coupled length $L_o$ equal to a wavelength at the center frequency. Next, the computed power plots of the output ports are obtained. The characteristics of the coupler are then adjusted such that the required lower band-edge frequency roughly corresponds to the frequency at which significant coupling appears for the first time. This adjustment is done by choosing an appropriate scalar multiplication factor for the $\boldsymbol{J}$ matrix, as discussed in Section II.

After this operation if it is found that the power plots are not approximately continuous (unbroken) within the band of interest, then better characteristics are obtained after running the optimization program for a short time (say 15 sec for a five-way coupler). The $\boldsymbol{e}$ obtained in this way is accepted as a good starting set of variables. It is necessary to make sure that the optimization is done at the initial frequency region of significant coupling and not in a later frequency region of coupling. A starting set of variables thus obtained reduces the computation time in the final optimization significantly.

## VI. Some Optimized Couplers and Their Characteristics

A number of couplers (starting from two-way up to nine-way) have been optimized successfully using the method presented here. The approximate CPU time required to perform the optimization and to produce the power and phase plots are (i) 30 sec for a two-way, (ii) 50 sec for a three-way, (iii) 80 sec for a four-way, and (iv) 110 sec for a five-way UCDC.

The characteristics for an optimized five-way equal power splitting coupler are presented in Fig. 4. Here in Fig. 4 one can observe the maximum deviation of 1.75 dB only within the octave bandwidth, in contrast to the 4 dB maximum deviation in the characteristics of [11].

Optimization of the above-mentioned couplers was performed for equal power distribution, although there should be no difficulty in optimizing for other distributions (consistent with the physics of a coupler). For seven-way and nine-way couplers, the characteristics of the outer lines exhibit less than an octave bandwidth. Besides, for these two cases the parameter values were found to be difficult to realize within reasonable length; at the same time the finger lengths exceed the resonance limits. As a result for a seven-way coupler a distribution with less power for the outer lines is taken. The computed characteristics of a seven-way coupler optimized for producing a half "sine"

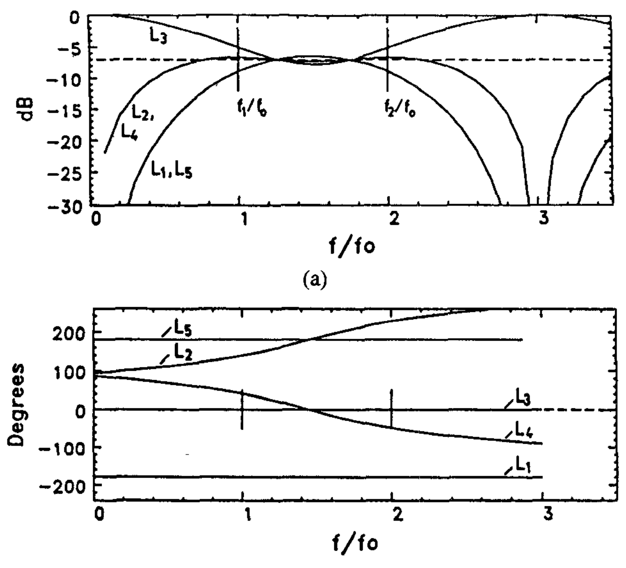


Fig. 4. Computed characteristics of a five-way UCDC with unit excitation at the input of line 3. (a) Power against frequency plots of output ports of the lines. (b) Relative phase against frequency plots of the output ports w.r.t. the output port of line 3. Band limits are shown for $\pm 1.75$ dB points. $L_1, L_2, \cdots, L_5$ are used to represent the characteristics of line 1, line 2, $\cdots$, line 5, respectively.

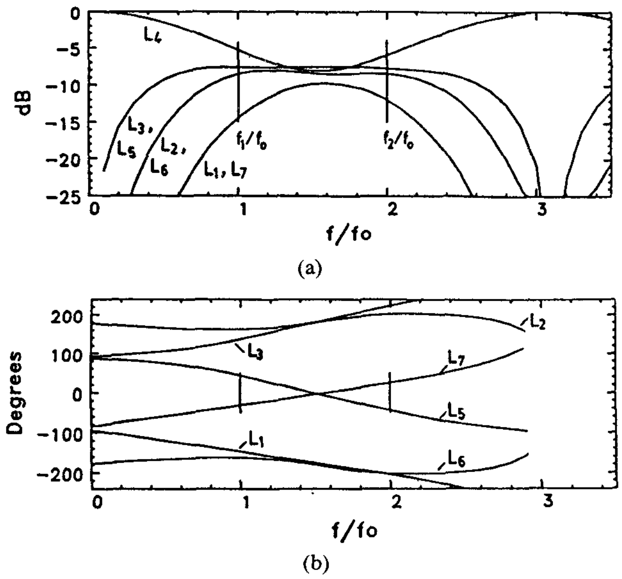


Fig. 5. Computed characteristics of an optimized seven-way UCDC with unit excitation at the input of line 4. (a) Power against frequency plots of the output ports of the lines. (b) Relative phase against frequency plots of the output ports w.r.t. the output port of line 4. Reference power levels for the output ports of lines 1 to 7 are $(\sin 30°)/s$, $(\sin 50°)/s$, $(\sin 70°)/s$, $(\sin 90°)/s$, $(\sin 110°)/s$, $(\sin 130°)/s$, $(\sin 150°)/s$ respectively, where $s = (\sin 30° + \sin 50° + \sin 70° + \cdot + \sin 150°)$. Band limits are shown for $\pm 2.0$ dB points. $L_1, L_2, \cdots, L_7$ are used to represent the characteristics of line 1, line 2, $\cdot$, line 7, respectively.

distribution of power are presented in Fig. 5. For a nine-way coupler the optimization has been done for a half sine pattern of power distribution. The achieved bandwidth in this case was less than an octave.

From the relative phase plots of the optimized couplers it may be observed that the phase characteristics of the lines adjacent to the direct line start from 90° at zero frequency and gradually change (almost linearly) with the increase in frequency. For the next adjacent lines this starts from 180°, and so on. Without altering the power characteristics, the phase characteristics of these couplers may be modified to produce a constant phase relationship within the operating band. The possible modifications are (i) 90° phase relationship for the coupled line output in a two-way coupler, (ii) +90° and −90° phase relationship of the coupled outputs (with respect to the direct line) in a three-way coupler, and (iii) +180°, −180°, +90°, and −90° phase relationship for lines 1, 5, 2, and 4, respectively, in a five-way coupler. These can be achieved by adding extra lengths of line at the end of the couplers.

From this investigation it appears that it is better to have the optimization, at first, done for power only. Next, after observing the phase characteristics of the coupler, one should perform the phase optimization or phase adjustments. The reason for this is that putting arbitrary restriction on phase condition at the beginning often causes difficulty in achieving a decent power optimization besides the delay in getting an optimized result.

## VII. A Practical Design Example

The five-way UCDC whose characteristics are presented in Fig. 4 was chosen for fabrication. The optimized $\boldsymbol{e}$ vector for this equal power splitting UCDC is $\boldsymbol{e}^t = (0.0650, 0.0556, 0.0603, 0.0650, 0.0556, -0.0052, -0.0032, -0.0032, -0.0052, 163.20)$. This means that the first five elements of this $\boldsymbol{e}$ are the diagonal elements and the next four elements are the off-diagonal elements of the tridiagonal $\boldsymbol{J}$ matrix. The coupled length is 163.2 mm.

### A. Obtaining Parameter Values and Dimensions from the Optimized e

The $\boldsymbol{J}$ matrix described above is, in fact, the matrix obtained after necessary adjustment of the center frequency of operation done by the scalar multiplication technique discussed in Section II. Also, necessary scaling was done by using

$$\boldsymbol{J} = \boldsymbol{Q}^t(\beta_{[1]} + \beta_o \boldsymbol{I})\boldsymbol{Q} = \boldsymbol{J}_{[1]} + \beta_o \boldsymbol{I}. \tag{13}$$

The subscript [1] is used to denote the matrices before scaling. This operation is done so that the scaled $\boldsymbol{J}$ produces physically realizable parameters. For this design it is desired to have 50 Ω coupled lines and 50 Ω terminations, so that $m_i = Z^c_{oi}/R_{ti} = 1$ is taken (Appendix I). The values of the coupled and uncoupled line parameters, including the interline coupling capacitances, are computed using the equations presented in Appendix I. With these line parameters, the physical dimensions of each line are then determined using the equations derived from the $ABCD$ matrices of a unit cell of a combline model. The combline model has a main line periodically loaded with susceptance $X$. The susceptance $X$ arises at the junction because of the fingers. A finger line and main line junction is treated as a microstrip T junction [21].

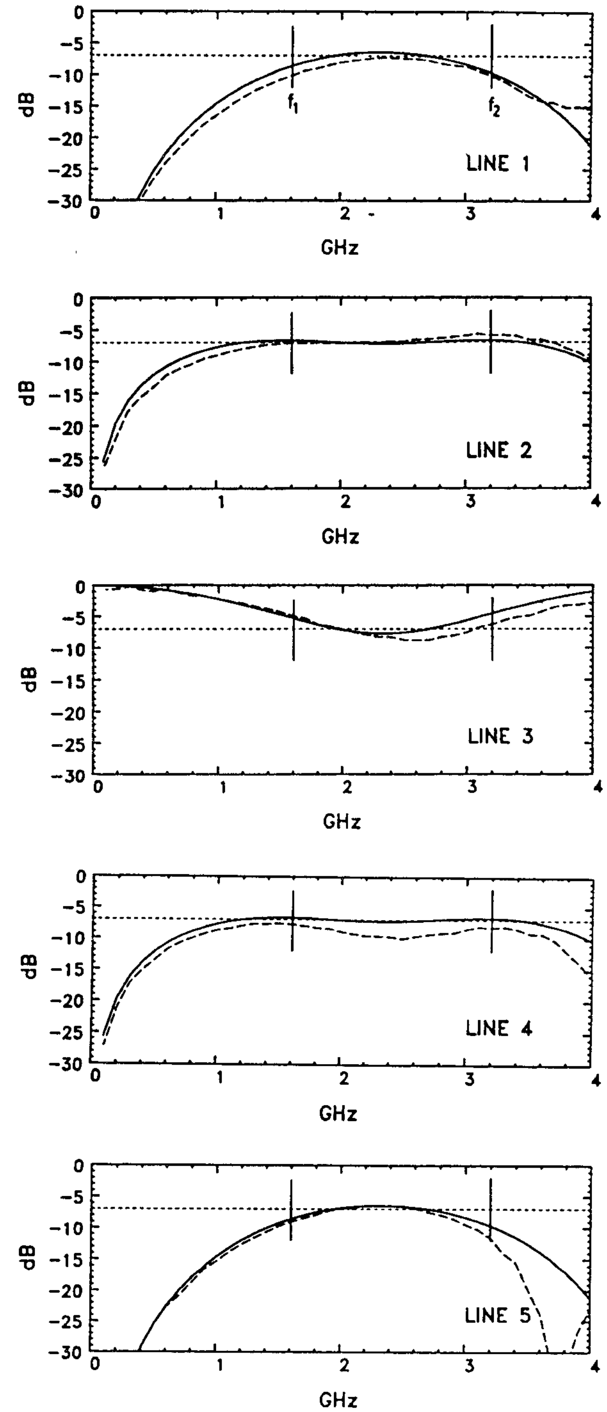


Fig. 6. Measured output power against frequency characteristics of the experimental five-way UCDC with unit excitation at the input of line 3. Band limits are shown for $\pm 1.75$ dB points. Back ports are terminated in 50 Ω. ---- measured; —— computed.

The finger overlap for a particular coupling capacitance is obtained using a plot of coupling capacitance against finger overlap. This plot was initially obtained by extending Garg and Bahl's [22] equations but was later modified based on the experimental observations.

After the computation one may find that, for a pair of lines, the available finger length is not sufficient compared to the required finger overlap. The finger lengths may then be altered by changing the $\boldsymbol{J}$ matrix using (13). For changing the finger overlap the interline coupling capacitances are changed by multiplying the coupled length and at the same time dividing the $\boldsymbol{J}$ matrix by the same factor. These operations do not change the characteristics.

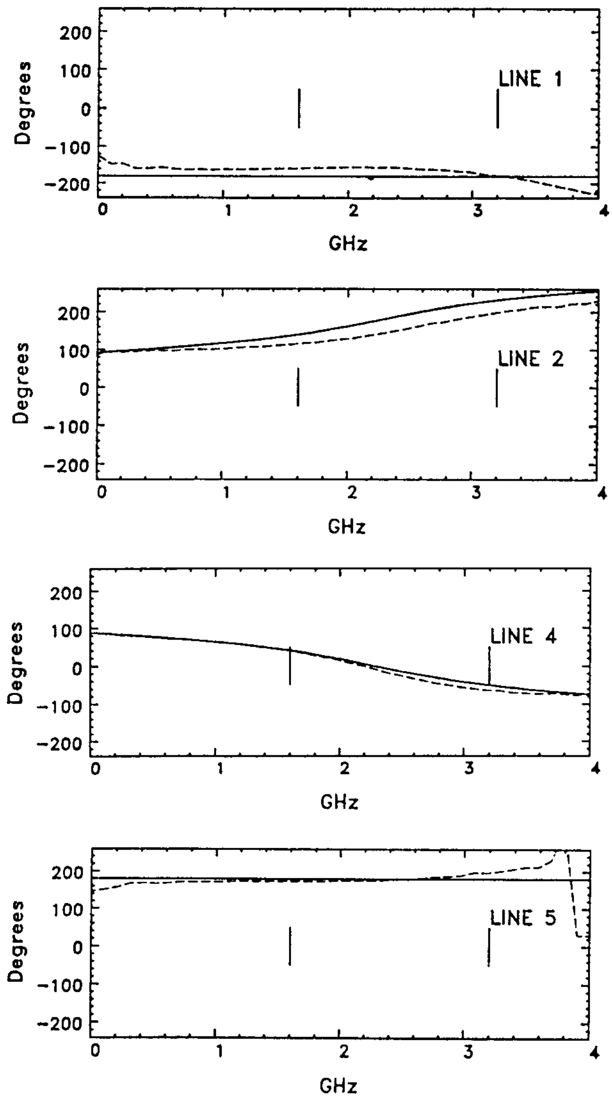


Fig. 7. Measured relative phase against frequency characteristics of the experimental five-way UCDC. Output of line 3 is taken as reference. ---- measured; —— computed.

The line parameters and some of the dimensions of the 1.6–3.2 GHz five-way UCDC obtained after computation as described above are presented in Appendix II.

### *B. Fabrication of the Five-Way UCDC*

The coupler was fabricated by usual photolithographic and etching techniques. A mask on rubylith film, prepared by a computer-operated scribing machine, is used for starting the work. Cu-clad 250 type GX-0600-55-11 copper laminate boards (made by 3M) having 1.5-mm-thick glass woven Teflon substrate ($\epsilon_r = 2.55$) were used for making the couplers in open microstip configuration. It may be mentioned here that the same length of connecting lines is required at the ports of the coupler. Otherwise the measured phase characteristics of the constructed coupler will differ from the computed characteristics. A photograph of

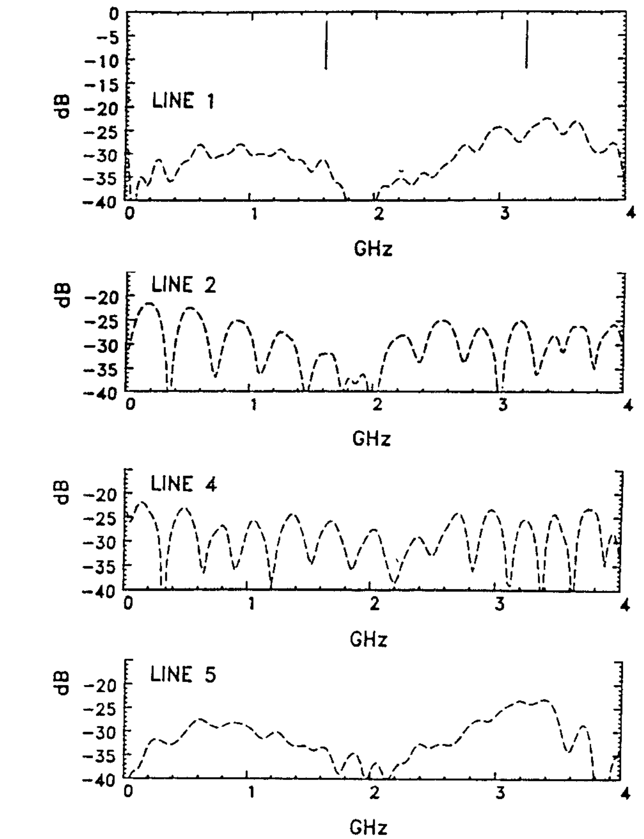


Fig. 8. Measured power against frequency plots of the back ports of the experimental five-way UCDC with unit excitation at the input of line 3.

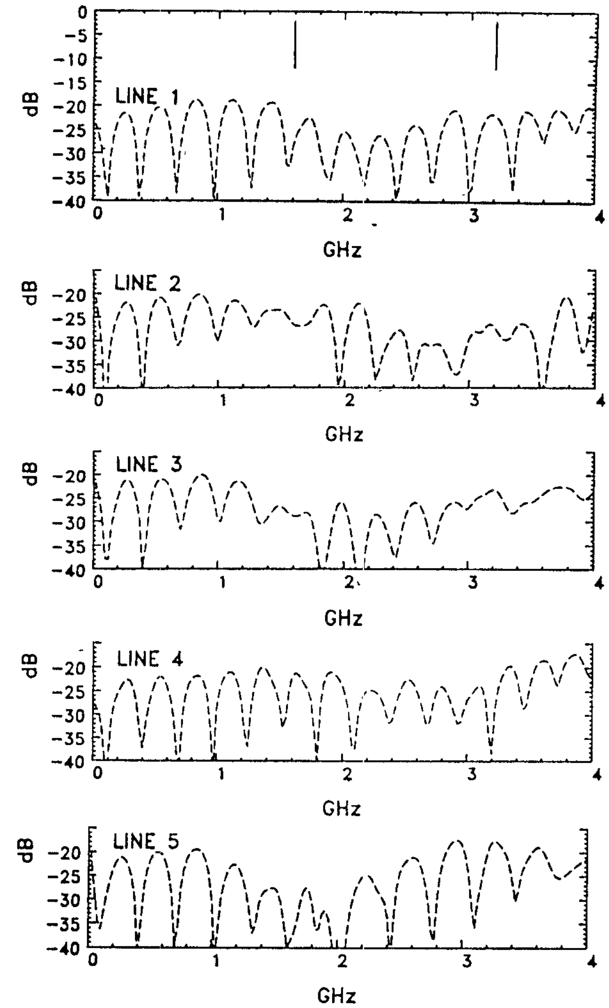


Fig. 9. Measured return loss of the lines of the experimental five-way UCDC.

the complete coupler fabricated using the design parameters of Appendix II is shown in Fig. 1.

### *C. Results of the Experimental Five-Way UCDC*

For obtaining the power and phase characteristics of the constructed coupler, an "in-house" time-domain network analyzer of the type described by Rigg and Carroll [16] was used. Frequency-domain measurement using modern network analyzers would have been advantageous for this measurement of couplers having several ports. However, the above-mentioned time-domain network analyzer [16] mainly comprises of a Tektronics fast rise time (25 ps) step generator (S-52 pulse generator head), a Tektronics 7504 sampling oscilloscope (with a loop through S-6 sampling head), an HP 9825A desktop calculator, and an interface unit between the calculator and the oscilloscope.

The measured power (dB) characteristics of the experimental five-way UCDC are presented in Fig. 6 and the measured phase characteristics are presented in Fig. 7. For the relative phase measurement, the output port of line 3 (middle line) was taken as reference. It may be observed from Figs. 6 and 7 that the measured results agreed well with the expected characteristics except for a small amount of imbalance in the power characteristics.

A number of couplers were made to identify the causes of deviations (imbalance in power splitting) and to improve the characteristics. From the measured characteristics of each of the modified couplers it has been observed that the deviations in the measured results were mainly due to the inaccurate phase velocities of the practical coupled lines. Such inaccuracy in the phase velocities of the coupled lines changes not only the coupled power levels but also the shape of the characteristics. This deviation in the realized phase velocities of the coupled lines causes significant deviation in the characteristics of a coupler having more than three lines. For multiway couplers, an improved and more accurate model analysis of the coupled comblines appears essential for obtaining improved characteristics.

The measured power characteristics of the back ports of the five-line UCDC are presented in Fig. 8. The maximum power within the operating band at the back port of lines 1, 2, 4, and 5 are $-25$ dB, $-25$ dB, $-24$ dB, and $-26$ dB, respectively. The return losses of the lines, measured using the same time-domain measurement technique, are presented in Fig. 9. From these plots it may be observed that within the operating band of frequencies the maximum VSWR's on lines 1 to 5 are 1.20, 1.15, 1.14, 1.20, and 1.29, respectively. However, the characteristic impedance measurement with the step generator in the time domain showed agreement within $\pm 1.5\ \Omega$.

## VIII. Conclusions

Improved optimization of the characteristics of a multiway UCDC is now possible by using the new $\boldsymbol{e}$ variables and the computer optimization technique presented in this paper. The use of the $\boldsymbol{e}$ vector as the set of variables makes it possible to examine the realizability of the coupler from the elements of the vector (i.e., the $\boldsymbol{J}$ matrix and the coupled length). The restriction on the $\boldsymbol{J}$ matrix automatically directs the optimization to a realizable structure and avoids search towards unrealizable area. In this method there is no need to normalize the vector containing the variables, in contrast to the previously used variables [11]. Altogether, this computer optimization with the $\boldsymbol{e}$ vector as variables is a powerful, easy-to-use, and useful technique for designing multiway UCDC's with an arbitrary number of lines.

From the observed behavior of UCDC's with up to five coupled lines, it may be concluded that an octave bandwidth can be obtained on an average, although certain lines (e.g., lines adjacent to the excited lines) exhibit wider bandwidth. The behavior of UCDC's having seven and more than seven coupled lines indicates that the outer lines exhibit less bandwidth than the lines closer to the excited line. From the results it is understood that the maximum attainable bandwidth can not readily be increased beyond an octave without incorporating some additional technique.

Besides using an open microstrip configuration for fabrication it is possible to use the triplate or shielded microstripline configuration. It is envisaged that the design technique presented here could possibly be extended to the design of couplers using dielectric waveguide gratings [18]–[20].

## Appendix I
## Equations for Obtaining Line Parameters from $\boldsymbol{J}$ Matrix

It has been shown in [11] that for a UCDC

$$\boldsymbol{J} = (\boldsymbol{B}_n + \boldsymbol{X}_n)/2$$

where

$$\boldsymbol{B}_n = \omega_1 \boldsymbol{R}_t^{1/2} \boldsymbol{C} \boldsymbol{R}_t^{1/2} \qquad \boldsymbol{X}_n = \omega_1 \boldsymbol{R}_t^{-1/2} \boldsymbol{L} \boldsymbol{R}_t^{-1/2}. \quad (14)$$

Here, $\omega_1 = 2\pi f_1$ and $\boldsymbol{R}_t$ may be taken as a diagonal termination matrix with $R_{ii}$ as the diagonal element corresponding to the $i$th line. $\boldsymbol{L}$ is the inductance matrix and is diagonal since the interline inductive coupling is negligible [8] for combline couplers. $\boldsymbol{C}$ is the tridiagonal (because of the nearest neighbor interaction) capacitance matrix. The diagonal elements of $\boldsymbol{C}$ are the self-capacitance $C_{ii}$ of the lines under coupled condition. The uncoupled self-capacitance $C_i$ may be computed from

$$C_i = C_{ii} - C_{i-1,i} - C_{i,i+1}. \quad (15)$$

The uncoupled and coupled characteristic impedances of the $i$th line are

$$Z_{0i}^u = \sqrt{(L_{ii}/C_i)} \quad \text{and} \quad Z_{0i}^c = \sqrt{(L_{ii}/C_{ii})}, \quad (16)$$

respectively.

The uncoupled and coupled phase velocities of the $i$th line are

$$v_{pi}^u = 1/\sqrt{(L_{ii}C_i)} \quad \text{and} \quad v_{pi}^c = 1/\sqrt{(L_{ii}C_{ii})}. \quad (17)$$

Using (14), (15), (16), and (17), it may be shown that

$$C_{ii} = (2J_{ii})/\{\omega_1 R_{ii}(1+m_i^2)\} \quad (18)$$

$$L_{ii} = (2J_{ii}R_{ii}m_i^2)/\{\omega_1(1+m_i^2)\} \quad (19)$$

and

$$C_{i,i+1} = 2J_{ii+1}/(\omega_1 R_{ii}). \quad (20)$$

Here, $m_i = Z_{0i}^c/R_{ii}$, $J_{ii}$ = the $i$th diagonal element of the $\boldsymbol{J}$ matrix, and $J_{i,i+1}$ = the off-diagonal term of the $\boldsymbol{J}$ matrix corresponding to the $i$th line.

## Appendix II
## Line Parameters and Dimensions of the Designed 1.6–3.2 GHz Five-Way UCDC

Coupled length $L_o = 163.2$ mm; dielectric constant $\epsilon_r = 2.55$; thickness of the substrate = 1.5 mm. Finger periodicity of the comblines = 2.4 mm; finger width = 1 mm; finger line impedance = 107 Ω.

| Line no. | Uncoupled impedance Ω | Coupled impedance Ω | Uncoupled velocity $\times 10^{11}$ mm/s | Coupled velocity $\times 10^{11}$ mm/s | Main line impedance Ω | Finger length mm | Coupling capacitance pF/m |
|---|---|---|---|---|---|---|---|
| 1 | 54.50 | 50 | 1.054 | 0.967 | 100.88 | 5.20 | $C_{12} = 32.75$ |
| 2 | 59.73 | 50 | 1.345 | 1.130 | 86.78 | 3.65 | $C_{23} = 20.24$ |
| 3 | 56.29 | 50 | 1.173 | 1.042 | 93.95 | 4.24 | $C_{34} = 20.24$ |
| 4 | 57.98 | 50 | 1.122 | 0.967 | 100.88 | 4.76 | $C_{45} = 32.75$ |
| 5 | 55.39 | 50 | 1.252 | 1.130 | 86.78 | 3.75 | |

Finger overlaps ($FO$): $FO_{12} = FO_{45} = 1.7$ mm, $FO_{23} = FO_{34} = 0.75$ mm.

## ACKNOWLEDGMENT

The author gratefully acknowledges the guidance of Prof. J. E. Carroll of the Cambridge University Engineering Department, Cambridge, U.K., in this project.


## REFERENCES


[1] E. M. T. Jones and J. T. Bolljahn, "Coupled-strip-transmission-line filters and directional couplers," *IRE Trans. Microwave Theory Tech.*, pp. 75–81, Apr. 1956.

[2] J. K. Shimizu and E. M. T. Jones, "Coupled transmission-line directional couplers," *IRE Trans. Microwave Theory Tech.*, pp. 403–410, Oct. 1958.

[3] L. Young, "The analytical equivalence of TEM-mode directional couplers and transmission-line stepped-impedance filters," *Proc. Inst. Elec. Eng.*, vol. 110, no. 2, pp. 275–281, Feb. 1963.

[4] R. Levy, "General synthesis of asymmetric multi-element coupled transmission-line directional couplers," *IEEE Trans. Microwave Theory Tech.*, vol. MTT-11, pp. 226–237, July 1963.

[5] T. C. Edwards, *Foundations for Microstrip Circuit Design*, New York: Wiley, 1981, pp. 129–171.

[6] S. A. Seward and S. B. Cohn, "Optimization of TEM mode tapered symmetric couplers," *Microwave J.*, vol. 28, no. 12, pp. 113–119, Dec. 1985.

[7] D. J. Gunton and E. G. S. Paige, "Directional couplers for gigahertz frequencies based on the coupling properties of two planar comb transmission lines," *Electron. Lett.*, vol. 11, no. 17, pp. 406–408, Aug. 21, 1975.

[8] D. J. Gunton, "Design of wideband codirectional couplers and their realization at microwave frequencies using coupled comblines," *Inst. Elec. Eng. J.*, MOA, pp. 19–30, Jan. 1978.

[9] J. E. Carroll and P. R. Rigg, "Matrix theory for *n*-line microwave coupler design," *Proc. Inst. Elec. Eng.*, pt. H., vol. 127, no. 6, pp. 309–314, Dec. 1980.

[10] P. R. Rigg and J. E. Carroll, "Three-line broadband codirectional microwave couplers using planar comb and herringbone microstrip lines," *Proc. Inst. Elec. Eng.*, pt. H, vol. 127, no. 6, pp. 315–322, Dec. 1980.

[11] B. A. Herscher and J. E. Carroll, "Design technique for multiport combline couplers with single port excited," *Proc. Inst. Elec. Eng.*, pt. H, vol. 129, no. 2, pp. 61–67, Apr. 1982.

[12] S. Islam and J. E. Carroll, "Warped-mode multiway combline directional couplers," *Proc. Inst. Elec. Eng.*, pt. H, vol. 133, no. 2, pp. 81–90, Apr. 1986.

[13] "NAGFLIB; 2082/1449: MK11: January 84" NAG manual, Chapter E04 — Minimizing or maximizing a function, Numerical Algorithms Group Ltd., Oxford, U.K.

[14] "NAGFLIB; 2075/1838: MK11: January 84" NAG manual, Chapter F02 — Eigenvalues and eigenvectors, Numerical Algorithms Group Ltd., Oxford, U.K.

[15] W. Murray, *Numerical Methods for Unconstrained Optimization*, London: Academic Press, 1972, pp. 87–106, 113–122.

[16] P. R. Rigg and J. E. Carroll, "Low-cost computer-based time-domain microwave network analyser," *Proc. Inst. Elec. Eng.* pt. H, vol. 127, no. 2, pp. 107–111, Apr. 1980.

[17] S. Islam, "Multi-way mode-interference and warped-mode microwave combline directional couplers," Ph.D. thesis, C.U. Engineering Department, Cambridge University, U.K., Aug. 1986.

[18] H. Shigesawa, "A completely theoretical design method of dielectric image guide grating in the Bragg reflection region," *IEEE Trans. Microwave Theory Tech.*, vol. MTT−34, pp. 420–426, Apr. 1986.

[19] P. K. Ikalainen and G. L. Matthaei, "Design of dielectric waveguide bandpass filters using parallel-coupled gratings," *IEEE Trans. Microwave Theory Tech.*, vol. MTT-34, pp. 681–689, June 1986.

[20] G. L. Matthaei, D. C. Park, Y. M. Kim, and D. L. Johnson, "A study of the filter properties of single and parallel-coupled dielectric-waveguide gratings," *IEEE Trans. Microwave Theory Tech.*, vol. MTT-31, pp. 825–835, Oct. 1983.

[21] E. O. Hammerstad, "Equations for microstrip circuit design," *in Proc. 5th European Microwave Conf.*, (Hamburg), 1975, pp. 256–260.

[22] R. Garg and I. J. Bahl, "Characteristics of coupled microstrip lines," *IEEE Trans. Microwave Theory Tech.*, vol. MTT-27, pp. 700–705, July 1979.


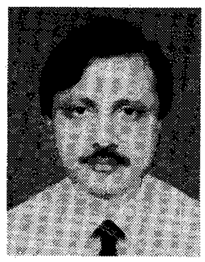


**Saiful Islam** received the B.Sc. Eng. (electrical) degree from the Bangladesh University of Engineering and Technology (BUET), Dhaka, Bangladesh, in 1975, the M.Sc. Eng. (electrical) degree from the same University in 1977, and the Ph.D. degree from Cambridge University, Cambridge, U.K., in 1986.

From 1975 to 1978 he was a Lecturer in the Electrical Engineering Department of BUET. During this period his research work was on microwave passive filters. From 1978 to 1983 he worked as an Assistant Professor in the Electrical and Electronic Engineering Department of BUET. From October 1983 to November 1986 he was on leave from BUET to complete his research work for the Ph.D. degree at Cambridge University. During this period he worked on different types of multiway microwave directional couplers. He is at present an Associate Professor in the Electrical and Electronic Engineering Department of BUET.

Dr. Islam is a fellow of the Institution of Engineers, Bangladesh, and an associate member of Institution of Electrical Engineers, London. His current research interests are in microwave directional couplers, filters, and multiplexers.